Molecular Host−Guest Energy-Transfer System with an Ultralow Amplified Spontaneous Emission Threshold Employing an Ambipolar Semiconducting Host Matrix

Stefano Toffanin,*,† Raffaella Capelli,† Tsyr-Yuan Hwu,‡ Ken-Tsung Wong,‡ Tobias Plötzing,§ Michael Först,§ and Michele Muccini†

Consiglio Nazionale delle Ricerche (CNR), Istituto per lo Studio dei Materiali Nanostrutturati (ISMN), via P. Gobetti 101, I-40129 Bologna, Italy, Department of Chemistry, National Taiwan University, Taipei 106, Taiwan, and RWTH Aachen University, Institut für Halbleitertechnik, Sommerfeldstrasse 24, 52074 Aachen, Germany

Received: September 17, 2009; Revised Manuscript Received: November 4, 2009

We report on the characteristics of a host−guest lasing system obtained by coevaporation of an oligo(9,9-diarylfluorene) derivative named T3 with the red-emitter 4-(dicyanomethylene)-2-methyl-6-(*p*-dimethylaminostyryl)-4*H*-pyran dye (DCM). We demonstrate that the ambipolar semiconductor T3 can be implemented as an active matrix in the realization of a host−guest system in which an efficient energy transfer takes place from the T3 matrix to the lasing DCM molecules. We performed a detailed spectroscopic study on the system by systematically varying the DCM concentration in the T3 matrix. Measurements of steady-state photoluminescence (PL), PL quantum yield (PLQY), time-resolved picosecond PL, and amplified spontaneous emission (ASE) threshold are used to optimize the acceptor concentration at which the ASE from DCM molecules takes place with the lowest threshold. The sample with a DCM relative deposition ratio of 2% shows an ASE threshold as low as 0.6 kW/cm^2 and a net optical gain measured by femtosecond time-resolved pump-and-probe spectroscopy as high as 77 cm^{-1}. The reference model system Alq_3:DCM sample measured in exactly the same experimental conditions presents an one-order-of-magnitude higher ASE threshold. The ASE threshold of T3:DCM is the lowest reported to date for a molecular host−guest energy-transfer system, which makes the investigated blend an appealing system for use as an active layer in lasing devices. In particular, the ambipolar charge transport properties of the T3 matrix and its field-effect characteristics make the host−guest system presented here an ideal candidate for the realization of electrically pumped organic lasers.

Introduction

Organic light emitting materials are attractive gain media for use in semiconductor lasers. Optically pumped laser action has been demonstrated in a broad range of materials in many different configurations with emission wavelengths covering the entire visible spectrum depending on the luminescent materials used. The demonstration of spectrally narrow emission in optically pumped thin organic films even in the presence of injecting metallic contacts is an important step toward the possibility of producing electrically pumped solid-state lasers from conjugated polymers and small molecules.[1]

The additional exciton quenching due to the presence of polarons increases the required performances of the lasing active material to be used in an electrically driven device. Lowering the ASE threshold diminishes the current density required to achieve electrically pumped lasing emission and reduces the polaron-induced absorption in the "gain" medium.[2] So great efforts are devoted to synthesizing new materials and to engineering new device structures with a lower ASE threshold and enhanced net gain coefficient. In this way, it would be possible to achieve lasing emission in real devices at an achievable current density even in the presence of residual exciton quenching and photon losses.

To realize efficient organic solid-state lasers, one can employ films of highly luminescent conjugated polymers[3] or alternatively utilize diluted dispersion of dyes or conjugated molecules embedded in a host matrix that can act either as a dispersive medium[4] or as a donor in energy transfer processes.[5]

Thin-film vacuum deposition of small organic molecules provides the advantage of a better control on the film morphology and the possible implementation in a multilayer device structure. Instead, conjugated polymers can be easily processable from solutions to realize simplified single-layer structures.

The use of a binary blend in which Förster energy transfer between an absorptive donor and an emissive acceptor takes place allows reducing the optical losses in the thin-film waveguides and decreasing the ASE threshold.

Indeed, the gain profile can be red-shifted with respect to the absorption band, and the low acceptor concentration (1−10%) minimizes concentration quenching. Although the benefits of energy transfer have been demonstrated, the way in which the energy transfer affects the ASE is still poorly understood.[6]

Apart from the enhanced optical performances of the blend system with respect to the single-material systems, in the case of a matrix with good charge transport properties the binary approach allows exploiting charge transport for the realization of opto-electronic organic devices such as organic light-emitting diodes and transistors and eventually electrically pumped organic lasers. Moreover, the matrix doping with small energy-gap molecules facilitates the implementation of energy-transfer

* Corresponding author. E-mail: s.toffanin@bo.ismn.cnr.it.
† Istituto per lo Studio dei Materiali Nanostrutturati (ISMN).
‡ National Taiwan University.
§ Institut für Halbleitertechnik.

10.1021/jp909003n
Published on Web 12/04/2009

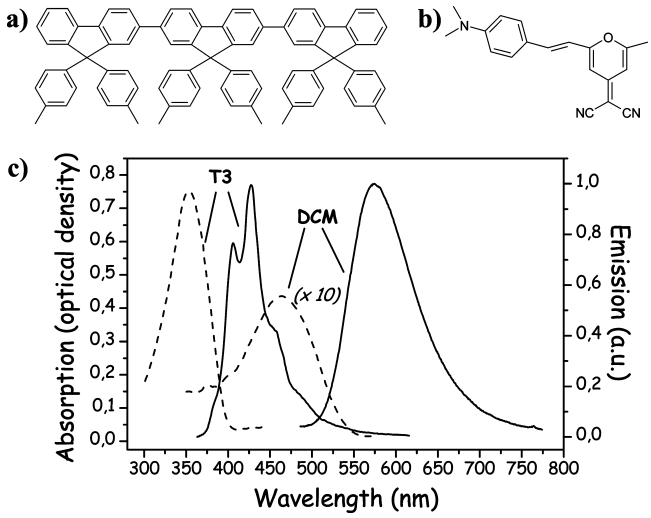

Figure 1. Chemical structure of (a) ter(9,9-diarylfluorene) (T3) and (b) 4-(dicyanomethylene)-2-methyl-6-(*p*-dimethylaminostyryl)-4*H*-pyran (DCM). (c) Absorption spectra (dashed line) and photoluminescence spectra (solid line) of a 10^{-5} M solution of DCM molecules dissolved in dichloromethane and of a 100 nm thick T3 film grown by thermal evaporation.

blends as charge-recombination and light-emission layers in multilayer-based opto-electronic devices.

Hereafter, we present a new host−guest lasing system whose optical properties are modulated by an efficient Förster energy transfer. The system is obtained by coevaporation of a oligodiarylfluorene derivative named T3 as the host material and the well-known red fluorescent dye 4-(dicyanomethylene)-2-methyl-6-(*p*-dimethylaminostyryl)-4*H*-pyran (DCM) as the guest material (see Figure 1 for molecular structures). T3 presents intriguing characteristics, such as high glass transition temperature, high thin-film PL quantum yield in pure blue,[7] ambipolar electrical characteristics in time-of-flight (TOF) measurements,[8] and field-effect charge transport.[9] Moreover, T3 ASE threshold and net gain are very competitive with respect to the most efficient polymeric and host−guest systems.[10]

We investigate how the guest concentration modifies the energy transfer dynamics and ASE properties of the host−guest system.[11] Steady-state and time-resolved photoluminescence spectroscopic study is performed to determine the guest concentration at which the ASE threshold is the lowest. Optical gain of the best performing T3:DCM blend is also measured by femtosecond pump-and-probe experiments.

The ASE characteristics of T3:DCM are compared with the case of the reference model system Alq_3:DCM that has to date the lowest ASE threshold among molecular binary host−guest systems.[12]

Since it is known that ASE threshold and gain values depend strongly on the experimental conditions used (exciting pulse duration, energy per pulse, illumination area), we performed the measurements on the T3:DCM and Alq_3:DCM systems in exactly the same experimental conditions to obtain a reliable direct comparison.

Experimental Methods

T3:DCM thin films of 150 nm nominal thickness were prepared by thermal evaporation under high vacuum onto quartz substrates kept at room temperature. The deposition rate was kept constant at 0.3 Å s^{-1} for each material. The different volume ratios of T3 and DCM were obtained by reducing the flux of one of the components on the substrate with a mechanical chopper placed in front of the sublimation source. The thin films of DCM dispersed in a PMMA matrix were obtained by spin coating an ethyl lactate solution of PMMA with 1% in weight of DCM.

UV−visible absorption spectra were recorded with a JASCO V-550 spectrophotometer, while PL spectra were collected in transmission by a Hamamatsu multichannel optical analyzer exciting the samples with 325 nm of a Kimmon He−Cd cw laser.

Time-resolved PL spectra were obtained exciting with the second harmonic of a Spectra-Physics femtosecond Ti:Sapphire laser at 385 nm and collecting PL with a Hamamatsu streak camera (time resolution ∼2 ps) after it was dispersed by a Chromex monochromator. A GG 400 cutoff filter and a spatial filter were used for preventing the excitation to reach the detector.

All the PL measurements were performed with the samples kept in vacuum (∼10^{-6} mbar) at room temperature.

PL quantum yield measurements were carried out in a Labsphere integrating sphere using as excitation sources either a Oxxius 375 nm laser diode or a 440 nm Kimmon cw He−Cd laser and a calibrated Hamamatsu multichannel optical analyzer as a detection system. All the measurements were performed in air.

The ASE properties of thin films were measured exciting with the third harmonic of a Q-switched Quantel Nd:YAG laser delivering 25 ns long pulses at 355 nm with a 10 Hz repetition rate. The laser intensity was adjusted before impinging on the sample by using neutral density filters, and the pumping energy was monitored using a calibrated laser energy meter (Scientech). An adjustable slit and a cylindrical lens were used to shape the laser beam into a strip with a width of 1 mm and a length of 4 mm. The films were pumped at normal incidence with the long axis of the pump beam perpendicular to the edge of the sample. The output signal was focused on a fiber-coupled Hamamatsu multichannel optical analyzer by a lens system. Measurements were performed in vacuum at 20 K.

Femtosecond time-resolved measurements were carried out in a standard pump-and-probe setup. The key component is a femtosecond regenerative Ti:sapphire amplifier which delivers trains of laser pulses of 40 fs duration at 800 nm central wavelength with pulse energies up to 3 mJ at a repetition rate of 1 kHz. For efficient optical excitation of the organic films, a nonlinear crystal was inserted into the pump beam to generate optical pulses at 400 nm wavelength via a second harmonic generation. To enable the measurement of time-resolved transmission changes over a broad wavelength range, the probe beam was fed into a sapphire crystal for supercontinuum generation by self-phase modulation (bandwidth ranging from 450 to 1100 nm). Pump-induced transmission changes of the organic film were recorded by suppressing each second pump pulse and recording the probe beam intensity after passing through the sample in a lock-in detection scheme. The spectral information was obtained by inserting a monochromator into the probe beam path between the sample and detector. In temporal transient measurements, the probe pulse was delayed with respect to the pump one by an optical delay line. Both the beams hit the sample under normal incidence, and the pump spot was kept much larger than the probe one to ensure probing in a homogenously excited region. The pump probe measurements were performed in vacuum at room temperature.

Results and Discussion

Steady-State Spectroscopic Properties. Förster theory[13] considers the weak coupling between the electronic and vibrational states of donors and acceptors suspended in a liquid solvent or a polymer matrix by dipole−dipole long-range interaction.

In the system we are considering the T3 thin-film matrix acts both as the donor and as the host, while the dispersed DCM molecules are the acceptors.

As can be seen from Figure 1, there is a large overlap between the emission spectrum of T3 thin film and the absorption spectrum of DCM dilute solution which is a necessary prerequisite to achieve efficient Förster resonance energy transfer in the host−guest system.

According to this theory, the rate of energy transfer from the excited donor (D) to the unexcited acceptor (A) is given by

$$K_{DA} = \frac{1}{\tau_D}(R_0/R_{DA})^6 \quad (1)$$

where τ_D is the lifetime of the donor in the absence of an acceptor; R_{DA} is the distance between the donor and the acceptor molecules; and R_0 is the Förster radius defined as the distance between the donor and acceptor at which energy transfer to the acceptor or decay on the donor occurs with equal probability. R_0 is expressed as

$$R_0^6 = \frac{9000(\ln 10)\langle k^2\rangle \phi_D}{128\pi^5 n^4 N_A} J \quad (2)$$

where Φ_D is the donor quantum yield in the absence of excitation energy transfer; n is the refractive index of the medium; N_A is Avogadro's number; and k^2 is the molecular orientation factor (for a fixed donor and a random distribution of fixed acceptors $\langle k^2\rangle = 0.476$[14]).

J is the overlap integral between the donor fluorescence and the acceptor absorption expressed in the frequency scale as

$$J = \frac{\int_0^\infty F_D(\bar{\nu})\varepsilon_A(\bar{\nu})d\nu/\nu^4}{\int_0^\infty F_D(\bar{\nu})d\bar{\nu}} \quad (3)$$

where $\varepsilon_A(\nu)$ is the molar decadic extinction coefficient of the acceptor at a wavenumber ν and $F_D(\nu)$ is the normalized intensity of donor fluorescence at ν.

From the overlap spectra of 10^{-5} M toluene solution of DCM molecules and a neat T3 thin film, we calculated an integral overlap of about 1.2×10^{-13} M^{-1} cm^2. Considering the T3 refractive index $n = 1.75$[7] and the measured T3 thin-film quantum yield of 47%, the estimation of the Förster radius is 36 Å.

In Figure 2a we report the absorption spectra of DCM:T3 blends obtained by increasing DCM concentration during the sublimation in vacuum. The neat T3 thin film and DCM dilute solution show absorption spectra peaked at ~383 and 463 nm, respectively. The blends spectra (which are normalized to the T3 peak in Figure 2a) are simply the linear combinations of the absorption of the pristine materials in the specific molar concentration, except for the slightly blue-shift in the DCM peak probably due to intermolecular interaction in the blend. T3 shows high absorbance at each dopant concentration, while DCM absorbance in the blend increases as expected with its concentration. The T3 absorption band is characteristic of the lowest $\pi-\pi^*$ transition of the central terfluorene chromophore, and the DCM absorption band is broad and featureless. From the absorption spectra, an estimation of the molar dopant concentration in the blend film can be obtained. The percentages of doping which identify the samples refer to the deposition flux of DCM with respect to T3 (see Experimental).

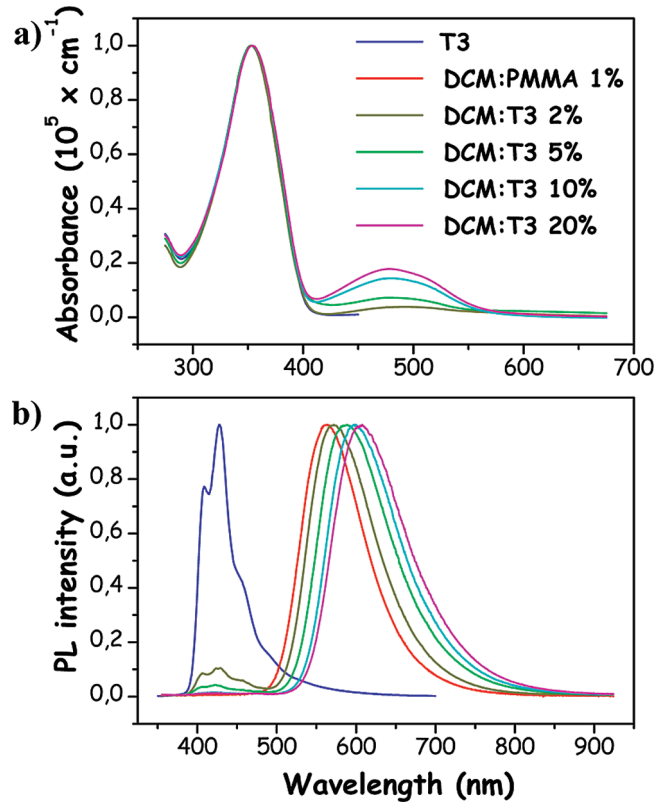

Figure 2. (a) Absorption spectra of thin films of different DCM:T3 blends with increasing DCM molar concentration and of T3 alone. All the spectra are normalized with respect to the T3 absorption peak alone for clarity. (b) Photoluminescence spectra of thin films of different DCM:T3 blends with increasing DCM molar concentration obtained by exciting the donor component. The spectra of the neat T3 thin film and of the solid solution of DCM dispersed in PMMA at 1% in weight are reported. Photoluminescence spectra are normalized with respect to their own maxima.

TABLE 1: Estimation of the DCM Molar Concentration (C_{DCM}) in the Blends from the DCM Deposition Rate Value during the Film Growth[a]

deposition rate	C_{DCM} [%]	R_{DA} [Å]
2%	14	12.6
5%	24	10.6
10%	38	9.1
20%	43	8.2

[a] The corresponding calculated donor−acceptor distances (R_{DA}) are reported.

By using the DCM molar decadic extinction coefficient in dilute solution, it is possible to calculate the guest molar fraction in the solid state samples assuming a homogeneous dispersion of noninteracting guest molecules in the host matrix. From the determination of the mean number of guest molecules per volume unit (n_A), we can obtain the nearest-neighbor distance in the three-dimension system by the expression $0.554/n_A^{1/3}$ derived by Chandrasekhar.[15] It is interesting to note (Table 1) that the mean distances (R_{DA}) calculated for all the DCM concentrations are lower than the Förster radius (R_0) obtained from spectroscopic data, thereby highlighting that in each

TABLE 2: Photoluminescence Quantum Yields (PLQY) of DCM:T3 Blends with Different DCM Concentrations Together with the Values Obtained from Neat T3 Thin Film and a Solid Solution of DCM Dispersed in PMMA at 1% in Weight[a]

	T3	2%	5%	10%	20%	DCM
PLQY @ 375 nm	0.46	0.25	0.12	0.07	0.06	0.7
PLQY @ 440 nm	-	0.4	0.21	0.1	0.08	0.6
ASE threshold (kW/cm^2)	4.4	0.6	1.1	2.8	3.8	-

[a] We selectively excite the donor or the acceptor components of the blends by using the 375 nm and the 440 nm wavelengths, respectively. We report also the values of the amplified spontaneous emission (ASE) thresholds for the blends and T3-alone thin films.

investigated sample the donor decay rate should be lower than the electronic energy transfer rate.

Attention should also be paid to the non-negligible integral overlap between the absorption and fluorescence spectra of the donor itself. This can lead to excitation energy transport within the donor.

In Figure 2b, the normalized photoluminescence (PL) spectra of the DCM:T3 blends at different concentrations are reported. The direct DCM emission is almost negligible at the excitation wavelength used (325 nm). T3-alone PL shows a vibronically resolved spectrum typical of polyfluorenes with the highest oscillator strength in correspondence of the 0−1 transition at 428 nm,[16] while the emission from DCM molecules dispersed in a PMMA matrix is broad since the full-width at half-maximum (fwhm) value is around 91 nm, featureless, and peaked around 562 nm. In the spectra of the composite films, there is the clear evidence of energy transfer from T3 to DCM, since by increasing DCM concentration the T3 component gradually disappears (in 10% and 20% samples, it is completely absent). For the 2% and 5% samples, we observe a slight blue-shift in the donor 0−1 PL peak due to DCM molecule reabsorption of the red wavelength portion of the donor fluorescence.[17]

As the guest concentration is increased, the DCM peak monotonically red-shifts from 570 nm for the 2% sample to 607 nm for the 20% sample, and the fwhm values increase from 98 nm for the 2% sample to 108 nm for the 20% sample. We can infer that DCM molecules dispersed in a solid matrix of T3 undergo an energy shift due to self-polarization for the more dilute samples and to real aggregate formation for the more concentrated ones. As the concentration of highly polar DCM molecules (dipole moment at ground state $\mu_g = 6.1$ D[18]) in relatively nonpolar T3 is increased, the distance between nearest-neighbor DCM molecules decreases, thereby increasing the local electrical field experienced by DCM molecules. In general, polar dopants, such as DCM, tend to arrange locally in oriented domains that minimize the overall energy of the system, causing a spectral red shift with respect to the isolated molecules.[19]

Indeed we observe that the DCM emission even in the 2% blend is red-shifted with respect to the emission of DCM dispersed at 1% in weight in a PMMA matrix.

Also, PLQY measurements seem to indicate the interaction among DCM molecules even at relatively low concentration. As can be seen in Table 2, although the PLQY of the DCM molecules dispersed in the PMMA matrix is around 70%, the quantum efficiency of the blend system is not improved with respect to that of the pure T3 host. The 2% sample shows the highest PLQY, while in the 10% and 20% samples it is severely quenched as expected when physical aggregates are formed. PLQY measurements exciting exclusively and directly the DCM molecules (440 nm excitation wavelength) show a similar trend. However, in the latter case the absolute PLQY are higher. This points to the fact that the energy transfer process affects the overall quantum yields of the blends.

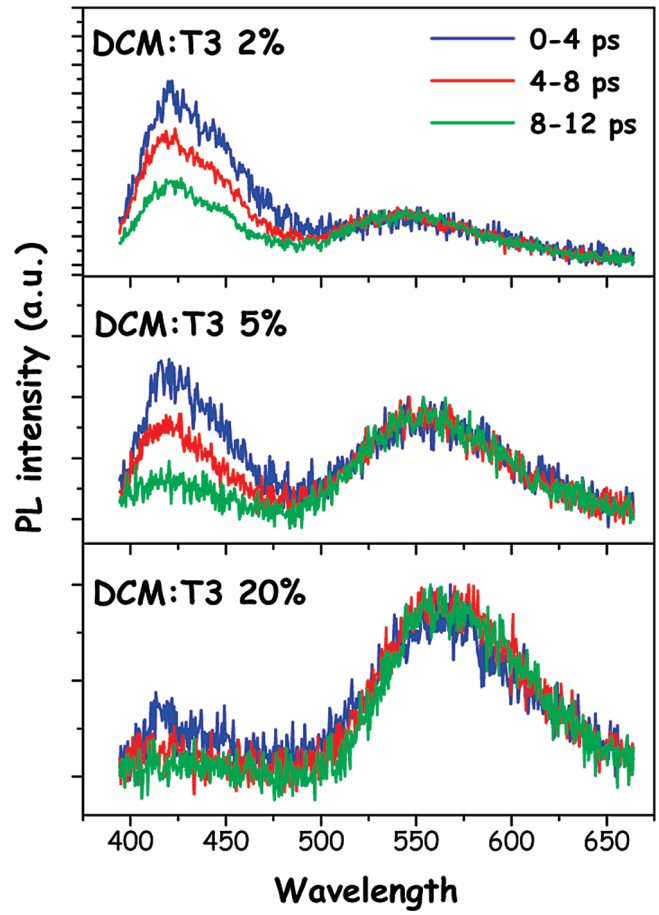

Figure 3. Transient PL spectra at different times for blends with different DCM concentrations. The spectra are normalized with respect to the DCM emission maximum.

Time-Resolved Energy Transfer. The transfer of excitation from the excited T3 chromophores to the dye molecules is monitored directly with time-resolved PL spectra. In Figure 3, the 2%, 5%, and 20% blend PL transients in three different temporal windows after excitation (0−4, 4−8, and 8−12 ps) are reported. At early times, only the 2% sample spectrum resembles almost completely the T3-alone one, apart from an instantaneous shift toward lower energy due to direct dyes excitation at this wavelength or to reabsorption effects. At later times, a relative enhancement of DCM emission occurs simultaneously with T3 emission quenching which reflects the energy transfer process. The entire dynamical process occurs over a time scale of 30 ps. By increasing DCM concentration, the blend PL spectra shift faster toward lower energy: for the 20% sample, the energy transfer is complete within 10 ps.

For a deeper investigation of the energy-transfer time evolution of the blend system, in Figure 4a we compare the PL decay collected at the T3 emission maximum in all the blend spectra with that of the neat T3 film.

The donor-alone temporal decay is well-fitted by a biexponential curve with an initial time constant of about 70 ps merging into a tail of 200 ps, being the amplitude of the fast component the larger one ($A \sim 0.53$). Since T3 thin-film dynamics is more appropriately described by a distribution of lifetimes rather than by a single time constant,[20] we define as the donor lifetime

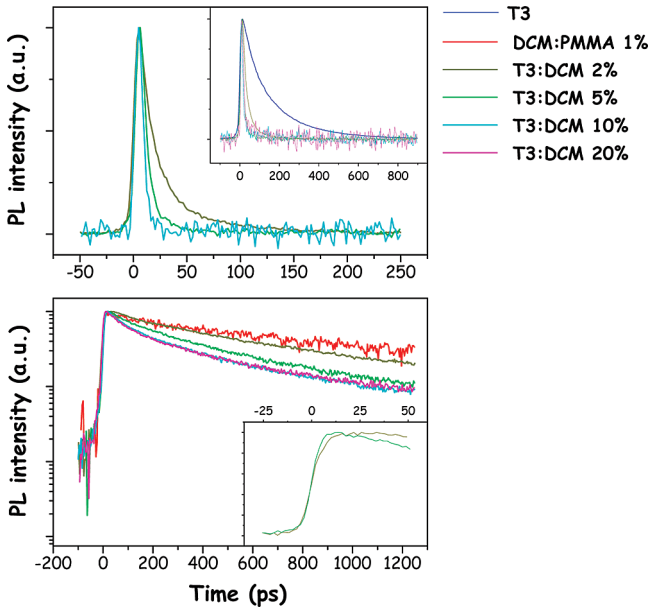

Figure 4. (a) DCM:T3 blends photoluminescence decay at the T3 0−1 vibronic wavelength for the 2%, 5%, and 10% blends. Neat T3 thin-film and 20% blend decay curves are reported in the inset. (b) DCM:T3 blends photoluminescence decay at the DCM maximum emission wavelengths. The decay of DCM dispersed in PMMA is also reported. 2% and 5% decay curves in a restricted time range are reported in the inset. The intensity is normalized at $T = 0$.

constant the weighted-average lifetime values obtained by the biexponential decay fitting.

From the time evolution of the neat T3 PL spectrum we can infer that within 10 ps after excitation there is a very fast transient spectral red-shift together with a slower inhomogeneous broadening of the 0−1 emission. It is likely that in competition with the decay to the electronic ground state a transfer process of electronic excitation within the density of states (DOS) distribution from high-lying to low-lying sites takes place.[21] Since it is energy- and time-dependent, this process is likely to happen through an energy dispersive incoherent hopping transfer mediated by a distance-dependent electronic coupling. Even if the inhomogeneous line width (taken as a rough estimation of the DOS) is quite large with respect to the thermal energy of the system at room temperature (~200 cm^{-1}), the relatively short excited state lifetimes prevent the observation of a clear energy-dependent relaxation process.[22]

By introducing dopant molecules in the matrix, T3 temporal decay becomes progressively more rapid as the dopant concentration is increased until the temporal resolution limit of the experimental setup is reached for the 10% and 20% samples.

We will now investigate in deeper detail T3 temporal dynamics of the 2% and 5% sample.

For the *2% sample*, the donor decay is again satisfactorily fitted by a biexponential curve (τ_1~14 ps, τ_2~63 ps) in which the amplitude of the fast component is much larger than the slow one (A_1~0.85, A_2~0.15). The weighted average lifetime is about a factor of 3 shorter than the value obtained from neat T3.

As we mentioned previously, the DCM:T3 blend can be described as a three-dimensional system with randomly distributed acceptor molecules in which the overlap integral (3) between the donor emission and the acceptor absorption spectra is not negligible and the donors and acceptors translational diffusion can be neglected. Therefore, the donor lifetime decay should be in principle described by the Förster ensemble-averaged nonexponential curve[23]

$$I(t) = \exp[-(at + bt^{1/2})] \tag{4}$$

with

$$a = 1/\tau_D; b = g\frac{4}{3}\pi^{3/2} n_A R_o^3/\tau_D^{1/2} \tag{5}$$

where τ_D is the fluorescence lifetime of the donor in the absence of the acceptors; n_A is the acceptor number density; R_0 is the Förster radius; and $g = (3\langle k^2\rangle/2)^{1/2}$ with $\langle k^2\rangle$ being the molecular orientation factor.

Using eq 4 as the interpolating curve, we find that the fit quality is not as good as for the biexponential one. From the fitting parameters, we calculate the donor lifetime τ_D as 70 ps and the acceptor number density n_A as 8.9×10^{18} cm^{-3}.

It is interesting to note that the donor fluorescence lifetime according to Förster fit is similar to the longer lifetime component obtained by fitting the data with two exponentials. Moreover, both the Förster lifetime constant (70 ps) and the weighted mean value of lifetime constants of the biexponential decay (22 ps) deviate significantly from the corresponding weighted mean value of the pure T3 (133 ps).

According to eq 4, the fluorescence is most rapid at the earliest times due to Förster transfer between close-lying donor−acceptor pairs. The decay rate of the host−guest system should asymptotically approach the host decay rate because the host dynamics is dominated at longer times by excited molecules that lie relatively distant from the acceptor molecules.[24] Taking into account the possible spectral exciton diffusion in the host material we described above, deactivation through diffusion-assisted energy transfer may provide an additional decay pathway that reduces the calculated host lifetime. This scenario is well corroborated by the data we collected. In the first few tens of picoseconds after excitation, most of the host photoluminescence is quenched due to the saturation of the guest nearest neighbors sites for energy transfer as the large amplitude of the fast component in the biexponential decay highlights. Nevertheless, diffusion is expected to reduce the rate of saturation of the nearest neighbors sites since excitons can travel in the host before transferring to the guest[25] as indicated by the discrepancy of the donor lifetime constant value obtained from Förster theory with respect to one of pure T3.

This hypothesis is sustained by the fact that the acceptor density obtained from the b parameter in Förster fitting, eq 5, of the PL decay is an order of magnitude smaller than the one calculated from absorption measurements (Table 1). Indeed the migration of the excitons in the host matrix would increase the overall energy transfer distance and result in an overestimation of the mean host−guest distance (R_{DA}).

Nevertheless, we also have to mention that from previous ellipsometry measurements on vacuum-deposited thin-film[7] T3 films exhibit rather significant uniaxial anisotropy with the optical axis along the surface normal. Given that the in-plane extinction coefficients are larger than out-of-plane coefficients, calculating n_A from normal-incidence absorption measurement with the assumption of an isotropic distribution of the host molecules can produce an overestimation of the guest numeric density and consequently a systematic underestimation of R_{DA}.

In the *5% sample*, the host temporal dynamics can be well fitted by monoexponential decay indicating the less dispersive nature of the energy transfer with this specific guest concentration. It is plausible that the mean donor−acceptor distance does not increase with time since the higher acceptor density

guarantees a rapid saturation of all the energy-transfer sites now homogeneously dispersed around the host molecules as the very fast and single lifetime constant indicates (~8 ps).

In Figure 4b we report the radiative decay profiles collected at the DCM emission maximum for each blend sample pumped at 385 nm. All the blend decay curves are only well-fitted by biexponential interpolation curves with the temporal dynamics getting faster as the guest concentration increases. We observe a general DCM emission quenching in the host−guest samples with respect to the solid solution of DCM molecules dispersed in PMMA in which an almost monoexponential dynamics behavior is present. Faster PL decay at higher concentrations coupled with a second slower time-constant component suggests that additional nonradiative decay pathways of the DCM excited state now compete with emission from isolated molecules.

This scenario is further confirmed by the comparison between the transient DCM PL within the first 20 ps and the quasi steady-state PL (see Supporting Information, Figure S2). With increasing DCM concentration in the blend the highly polar DCM molecules start first by interacting through dipolar interaction in the less polar T3 matrix and then by forming weakly emissive aggregates.[26]

The 10% and 20% samples present identical spectroscopic features, i.e., emission wavelengths, PL quantum yields, and lifetime constants. This can highlight that a guest concentration exists, above which the electronic characteristics of the emitting aggregates in the T3 matrix reach an equilibrium value.

As can be inferred from the inset in Figure 4b, for the 2% and 5% samples the DCM signal shows an initial rise in intensity at early times reaching a maximum value, whereupon the signal starts its natural decay. The initial rise is attributed to the energy transfer process from the T3 host to the DCM guest molecules, resulting in an increasing population of guest molecules in the excited state. The amount of time required for buildup of guest molecules in the excited state (referred to as the rise time τ_{rise}) decreases as the guest concentration increases. Fitting the guest transient signal by a negative exponential function in the temporal range before guest PL decay starts,[24] it is possible to achieve an estimation of τ_{rise}: around 7 and 3 ps for 2% and 5% samples, respectively.

We can estimate the energy transfer rate immediately after the host excitation from the guest rise time through the expression $k_{ET} = \tau_{rise}^{-1} - \tau_{DA}^{-1}$ in which τ_{DA} refers to the donor single lifetime constants in the blend. The energy transfer rates we calculated for the 2% and 5% blends are 57 and 118 GHz.

Both these values are higher than the ones obtained from the Förster relation, $k_{ET} = \tau_{DA}^{-1} - \tau_{D}^{-1}$, in which donor lifetimes in the blend (τ_{DA}) and alone (τ_{D}) are taken into account. In particular, for the 2% blend the energy transfer rate obtained from the guest rise time is much higher than the "steady-state" value, indicating that the energy transfer between the closest-lying donor−acceptor pairs dominates the dynamics at the earliest times following excitation. This is a clear signature of the Föster-like nature of the energy transfer process for the 2% blend.

Complementary information on the energy transfer dynamics between host and guest molecules can be obtained from femtosecond time-resolved pump-and-probe spectroscopy since it is able to monitor the optical properties of the blend at time resolution less than 100 fs. In these experiments, stimulated emission (and not spontaneous emission as in PL measurements) is probed, allowing for the direct determination of optical gain within the organic film. In Figure 5 the transmittance variation of the white light probe pulse after passing through the 2% sample is displayed as a function of detection wavelength and time delay after optical excitation. Blue colored regions indicate a decrease of transmittance due to the pump pulse, whereas in red colored regions the probe pulse is amplified during its propagation through the film after the optical excitation of the host molecules. At negative time delays, i.e., the probe pulse hits the sample before the pump pulse, no significant change in transmittance is observed. The slight enhancement around the PL emission maximum at 600 nm can be ascribed to the residual spontaneous emission of the excited DCM molecules, which is collected by the detection system. At zero time delay an

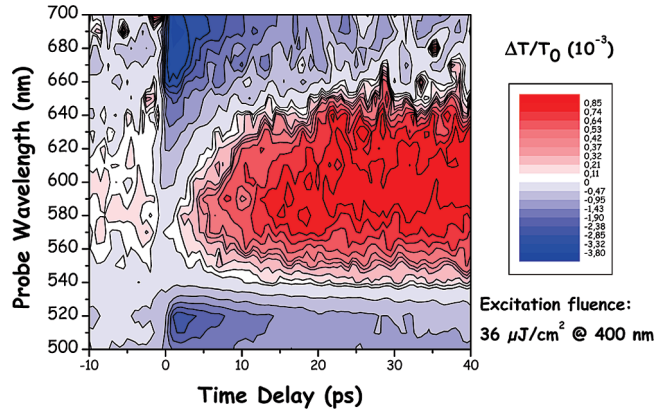

Figure 5. Spectrally and temporally resolved transmittance change of the 2% DCM:T3 sample obtained in a femtosecond pump and probe measurement. The sample is excited by a 40 fs laser pulse at 400 nm central wavelength and a fluence of 36 μJ/cm^2. Red colored regions indicate optical gain, whereas blue regions indicate pump-induced additional loss.

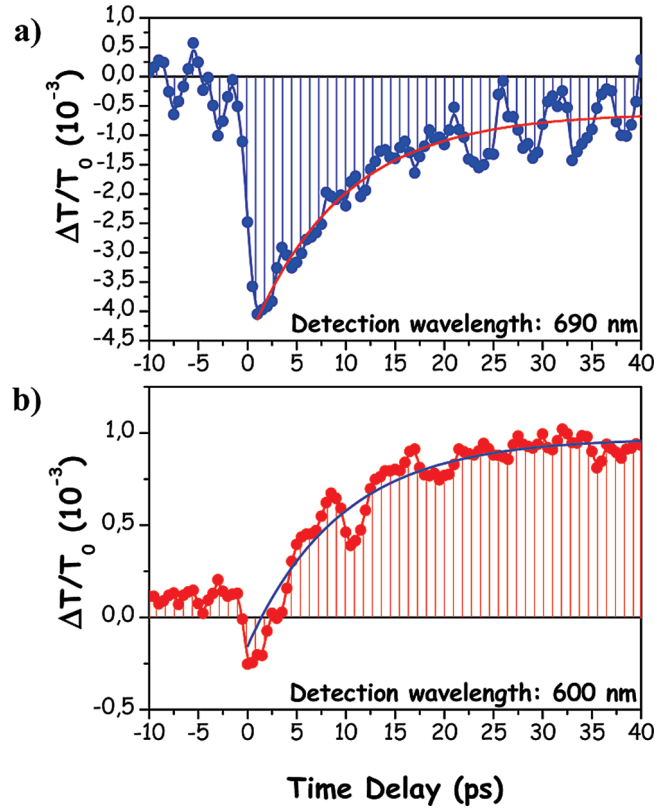

Figure 6. Temporal cross sections of Figure 5. (a) Cross section at 690 nm, where a maximum absorption increase is observed (blue circles). (b) Cross section at a maximum gain wavelength of 600 nm (red circles). Exponential fits to the data for positive time delays (red (a) and blue (b) solid lines) are also reported.

instantaneous decrease in transmittance occurs for all wavelengths, which subsequently vanishes in the long and short wavelength regions of the graph. In the center wavelength region, a transient transmittance increase with its maximum at ~40 ps is present. For a more detailed analysis, temporal cross sections of the probe transmittance variation at specific wavelengths of 690 and 600 nm are displayed in Figure 6. In the latter case (Figure 6a), the probe pulse transmittance through the sample abruptly drops when the sample is excited by the pump pulse. Since the pump energy is predominantly absorbed by the T3 host molecules, the sudden drop in transmittance has to be attributed to an excited state absorption within the T3 matrix. At these early time delays, the DCM guest molecules are not yet excited. When the energy is subsequently transferred from T3 to DCM molecules by Förster energy transfer, the number of excited T3 molecules decreases and hence the transmittance change recovers to zero exponentially. From a numeric fit, a relaxation constant of 9.5 ps is found.

In Figure 6b, the temporal dynamics of the probe transmittance at the maximum PL emission wavelength of DCM is reported. The short drop in probe pulse transmittance at zero time delay is again attributed to excited state absorption in T3. Admittedly, at this wavelength the increasing number of excited DCM molecules leads to an amplification of the probe light and quickly overcompensates the absorption, leading to a positive transmission change. An exponential fit to the build-up of gain provides exactly the same time constant of $\tau_{rise} =$ 9.5 ps, supporting the above sketched assumptions. Furthermore, the time constant τ_{rise} is in good agreement with the value of 7 ps obtained from time-resolved PL measurement.

ASE Threshold. In Table 2 we report the ASE pump intensity thresholds with varying DCM concentrations in the blends together with the T3-alone value. The ASE threshold is defined as the pump intensity at which the fwhm is reduced to half the fwhm of the PL at low pump intensity.

The ASE peaks located always in the DCM emission region regardless of the dopant concentration reveal that upon T3 molecule excitation the energy transfer toward DCM molecules dominates over the T3 stimulated emission process. Considering the laser exciting pulse (25 ns at fwhm) as steady state compared with the energy transfer and radiative decay time scale in the system, we can assign the energy transfer rate in the first 20 ps in the 2% sample as an inferior limit for the ASE rate value in the neat T3 thin film.

Increasing DCM concentration, the energy transfer rate seems to increase, while the ASE threshold does not reduce. It is worth noting that in the ASE spectrum of the 20% sample the DCM ASE peak is much broader and the T3 emission component is clearly visible (but completely absent in the steady-state transmission spectrum) as if T3 and DCM ASE processes were competing (Figure 7). Moreover, the lowest ASE threshold value is found in correspondence of the 2% sample, indicating that the spontaneous emission guided through the exciting stripe is very sensitive to the aggregation state of the emitting molecules.

The overall trend of ASE thresholds at different DCM concentrations can be explained with respect to the spectroscopic parameters we measured. From the acceptor quantum yield (Φ_A) and lifetime constant (τ_A) in the blend, it is possible to determine the radiative decay rate ($k_r = \Phi_A/\tau_A$). Here, k_r is related to Einstein's B coefficient through the relation $B \sim (c^3/8\pi h\nu_0^3)k_r$ where h is Planck's constant; ν_0 is the frequency of light; and c is the velocity of light. Since the ASE threshold is inversely proportional to the B coefficient, we would expect a large k_r to result in a low ASE threshold.[27] Indeed, the 2% blend presents

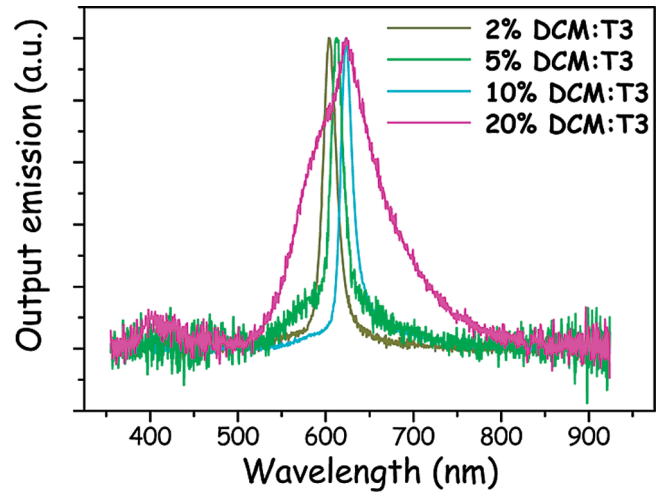

Figure 7. Normalized DCM:T3 blends emission spectra collected from the edge of a 4 mm^2-wide excitation stripe. The pump intensity is higher than the ASE threshold.

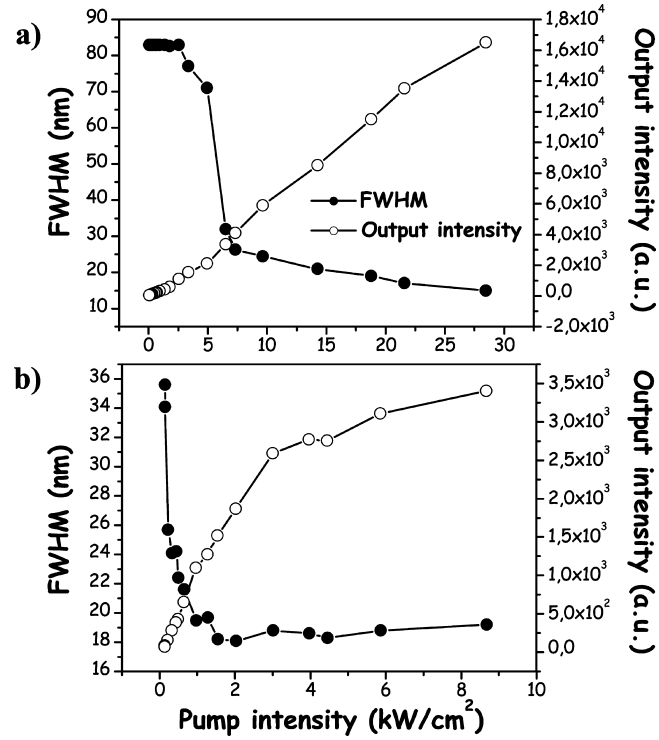

Figure 8. Dependence of the photoluminescence intensity (open circles) and full-width at half-maximum (solid circles) on the excitation pump intensity for a 300 nm thick thin film of 2% DCM:Alq_3 blend (upper) and a 150 nm thick thin film of 2% DCM:T3 blend (lower).

the highest acceptor radiative decay together with the lowest ASE threshold.

This value corresponding to about 0.6 kW/cm^2 is not only 7 times lower than the T3-alone ASE threshold value but also almost an order of magnitude lower than the ASE threshold value we measured under the same experimental conditions for the model system DCM:Alq_3 (Figure 8). It is important to note that the ASE measurements on the two different host−guest systems are carried out using the same experimental setup so that the extracted ASE threshold values can be reliably compared.

Moreover, from the pump and probe measurements on the 2% sample, it is possible to extract a maximum gain of 77 cm^{-1} for the investigated pump fluence of 36 μJ/cm^2 (Figure 6b).

Differently from transient absorption measurements, geometrical and physical constraints in the ASE measurements are very close to those of real waveguide lasers. Moreover, using a laser source with a 10 Hz repetition rate, triplets accumulation and undesirable thermal effects are prevented since after excitation the gain medium is given time to recover prior to the arrival of the next excitation pulse.[28] Since we are dealing with host−guest systems, it is important that the laser pulse amplitude is much longer (in the order of nanoseconds) than the energy transfer and nonlinear nonradiative processes time scale so that the depletion of the excited DCM molecules can occur via ASE.[29]

It can be seen that the ASE peak is located in the low-energy side of the PL spectrum because the higher net gain always takes place at the peak far from the absorption edge that would introduce self-absorption.[30] We also note that the shift of the ASE peak with respect PL peak position decreases with increasing DCM concentration. Since the films present nominally the same thickness (about 150 nm), it is likely that in highly doped samples the ASE wavelength could be affected by excited-state absorption (reducing net gain at larger wavelengths) rather than amplification of different modes due to cavity effects. Consistently photoinduced absorption measurements on the milliseconds time scale carried out on T3-alone thin film show a broad peak centered at 690 nm that is assigned to triplet−triplet absorption from the lowest T_1 to a generic upperlying T_n state.[31]

Conclusions

In conclusion, we investigated the photophysical properties of the new lasing DCM:T3 system in which an efficient Förster energy transfer takes place from the ambipolar semiconducting matrix T3 to the lasing molecule DCM. By varying the guest concentration, we studied the energy transfer dynamics by steady state and picosecond time-resolved spectroscopy finding out that the nonradiative energy transfer is Förster-like only for the lowest guest concentration sample. For higher guest concentrations, the energy transfer becomes much faster, but the overall dynamics is ruled by the guest interaction and aggregation.

The mirrorless lasing measurements performed on the blends reveal that the lowest ASE threshold is presented by the blend in which the guest aggregation is almost negligible and the energy transfer is incomplete.

The ASE threshold of the 2% DCM:T3 system is the lowest reported to date for a binary energy-transfer system and is one order of magnitude lower than that of the 2% DCM:Alq_3 model system measured in the same experimental conditions.

This property, coupled to the ambipolar charge-transport characteristics of the T3 matrix, makes this blend a very attractive candidate to be used as a gain medium for the fabrication of organic solid-state lasers. Indeed, reducing the ASE threshold to ultralow values is one of the key parameters that allows reducing the required current density and the polaron−exciton interaction in the gain medium of electrically pumped devices.

Acknowledgment. This work was supported at Bologna by EU under projects FP7-ITC-248052 (PHOTO-FET) and EU-FP6-Marie Curie-035859 (BIMORE) and by Italian Ministry MIUR under Projects FIRB-RBNE033KMA, FIRB-RBIP06JWBH (NODIS), and FIRB-RBIP0642YL (LUCI). The authors thank M. C. Ramon for the help in the ASE threshold measurements of DCM:Alq_3 sample and R. Zamboni and G. Ruani for stimulating discussions.

Supporting Information Available: Figures S1 and S2. This material is available free of charge via the Internet at http://pubs.acs.org.

References and Notes

(1) Yokoyama, D.; Nakanotani, H.; Setoguchi, Y.; Moriwake, M.; Ohinishi, D.; Yahiro, M.; Adachi, C. *Jpn. J. Appl. Phys.* **2007**, *46*, L826–L829.
(2) Yamamoto, H.; Kasajima, H.; Yokoyama, W.; Sasabe, H.; Adachi, C. *Appl. Phys. Lett.* **2005**, *86*, 83502–83503.
(3) Xia, R.; Heliotis, G.; Bradley, D. D. C. *Appl. Phys. Lett.* **2003**, *82*, 3599–3601.
(4) Nakanatomi, H.; Akiyama, S.; Ohnishi, D.; Moriwake, M.; Yahiro, M.; Yoshihara, T.; Tobita, S.; Adachi, C. *Adv. Funct. Mater.* **2007**, *17*, 2328–2335.
(5) Zhang, D.; Ma, D. *Appl. Phys. B: Laser Opt.* **2008**, *91*, 525–528.
(6) Sheridan, A. K.; Buckley, A. R.; Fox, A. M.; Bacher, A.; Bradley, D. D. C. *J. Appl. Phys.* **2002**, *92*, 6367–6371.
(7) Lin, H. W.; Lin, C. L.; Chang, H. H.; Lin, Y. T.; Wu, C. C.; Chen, Y. M.; Chen, R. T.; Chien, Y. Y.; Wong, K. T. *J. Appl. Phys.* **2004**, *95*, 881–886.
(8) Wu, C. C.; Liu, T. L.; Hung, W. Y.; Lin, Y. T.; Wong, K. T.; Chen, R. T.; Chen, Y. M.; Chien, Y. Y. *J. Am. Chem. Soc.* **2003**, *125*, 3710–3711.
(9) Oyamada, T.; Chang, C. H.; Chao, T. C.; Fang, F. C.; Wu, C. C.; Wong, K. T.; Sasabe, H.; Adachi, C. *J. Chem. Phys. C* **2007**, *111*, 108–115.
(10) Lin, H. W.; Lin, C. L.; Wu, C. C.; Chao, T. C.; Wong, K. T. *Org. El.* **2007**, *8*, 189–197.
(11) Camposeo, A.; Mele, E.; Persano, L.; Pisignano, D.; R. Cingolani, R. *Phys. Rev. B* **2006**, *73*, 1652011–1652017.
(12) Lu, W.; You, H.; Fang, J.; Ma, D. *Appl. Opt.* **2007**, *46*, 2320–2324.
(13) Förster, T., *Modern Quantum Chemistry, Part 2: Action of Light and Organic Molecules*; Academic: New York, 1982.
(14) Rozman, I. M. *Opt. Spectrosc.* **1958**, *4*, 536–538.
(15) Chandrasekhar, S. *Rev. Mod. Phys.* **1943**, *15*, 86.
(16) Salbeck, J.; Yu, N.; Bauer, J.; Weissörtel, F.; Bestgen, H. *Synth. Met.* **1997**, *91*, 209–215.
(17) Jena, K. C.; Bisht, P. B. *Chem. Phys.* **2005**, *314*, 179–188.
(18) Kwak, G.; Okada, C.; Fujiki, M.; Takeda, H.; Nishida, T.; Shiosaki, T. *Jpn. J. Appl. Phys.* **2008**, *3*, 1753–1756.
(19) Farchioni, R. Grosso, G. *Organic Electronic Materials*; Springer-Verlag: Berlin Heidelberg, 2001.
(20) Mollay, B.; Lemmer, U.; Kersting, R.; Mahrt, R. F.; Kurz, H.; Kauffmann, H. F.; Bässler, H. *Phys. Rev. B* **1994**, *50*, 10769–10779.
(21) Meskers, S. C. J.; Hübner, J.; Oestreich, M.; Bässler, H. *J. Phys. Chem. B* **2001**, *105*, 9139–9149.
(22) Hildner, R.; Lemmer, U.; Scherf, U.; Köhler, J. *Chem. Phys. Lett.* **2006**, *429*, 103–108.
(23) Lee, M.; Tang, J.; Hochstrasser, R. M. *Chem. Phys. Lett.* **2001**, *344*, 501–508.
(24) Wolak, M. A.; Melinger, J. S.; Lane, P. A.; Palilis, L. C.; Landis, C. A.; Delcamp, J.; Anthony, J. E.; Kafafi, Z. H. *J. Phys. Chem. B* **2006**, *110*, 7928–7937.
(25) Lyons, B. P.; Monkman, A. P. *Phys. Rev. B* **2005**, *71*, 2352011–2352015.
(26) Scholes, G. D.; Jordanides, X. J.; Fleming, G. R. *J. Phys. Chem. B* **2001**, *105*, 1640–1651.
(27) Aimono, T.; Kawamura, Y.; Goushi, K.; Yamamoto, H.; Sasabe, H.; Adachi, C. *Appl. Phys. Lett.* **2005**, *86*, 711101–711103.
(28) Samuel, I. D. W.; Turnball, G. A. *Chem. Rev.* **2007**, *107*, 1272–1295.
(29) Kallinger, C.; Riechel, S.; Holderer, O.; Lemmer, U.; Feldmann, J.; Berleb, S.; Mückl, A. G.; Brütting, W. *J. Appl. Phys.* **2002**, *91*, 6367–6370.
(30) McGehee, M. D.; Hegeer, A. J. *Adv. Mater.* **2000**, *12*, 1655–1668.
(31) Cabanillas-Gonzales, J.; Sciascia, C.; Lanzani, G.; Toffanin, S.; Capelli, R.; Ramon, M. C.; Muccini, M.; Gierschner, J.; Hwu, T. Y.; Wong, K. T. *J. Phys. Chem B* **2008**, *112*, 11605–11609.

JP909003N